CrossMark
click for updates

Glycyrrhizin modulates ER stress-induced UPR and concomitant mitochondrial dysfunction and activation of NF-κB in alcohol and cerulein-induced pancreatitis in rats

Sarmishta Srikantam[1], Geetha Arumugam[2*]

[1]Department of Biochemistry, Bharathi Womens College, Chennai, India.
[2]Principal, Dr. Ambedkar Government Arts College, Chennai, India.

ARTICLE INFO

ABSTRACT

Chronic pancreatitis (CP), a long-lasting pancreatic inflammatory illness, results predominantly from prolonged alcohol abuse. No standardized treatment exists so far. This investigation studies the effect of glycyrrhizin (GZ) on ethanol (EtOH) and cerulein (Cer)-induced pathology in the pancreas of male albino Wistar rats. Endoplasmic reticulum (ER) stress, mitochondrial damage, and activation of nuclear factor-κB (NF-κB) are the important pathomechanisms of CP. Rats were sorted as follows: Group 1 (control) and group 2 (GZ control) were given normal diet for the total period of 5 weeks, whereas group 3 (EtOH + Cer) and group 4 (EtOH +Cer+ GZ) were given alcoholic diet (0%–36%) for 4 weeks and Cer (20 µg/kg of body weight, IP) three times a week for the last 3 weeks to induce CP. Group 2 and group 4 rats were also given GZ (10 mg/kg of body weight, oral) from third week. GZ co-administration modulated ER stress by downregulating mRNA expression of unfolded protein response components like activating transcription factor 4, 78 kDa glucose-regulated protein (GRP78), CCAAT-enhancer-binding protein homologous protein (CHOP), X-box binding protein 1 and the inflammatory mediator, NF-κB. In addition, GZ ameliorated cellular oxidative stress. Measurements of calcium, complex-1 activity, and oxidative stress [including 4-hydroxynonenal (4-HNE)] in mitochondria substantiated the protective effect of GZ against mitochondrial dysfunction. Applying spearman's rank correlation (rs), a significant positive correlation between GRP78 versus 4-HNE ($p < 0.05$) and CHOP versus mitochondrial calcium ($p = 0.00$) was proved, which could indicate that ER stress and mitochondrial dysfunction act in concert to cause the pathobiology in CP. It can be concluded that GZ exhibits pancreato-protective effect against CP likely by targeting ER stress, NF-κB signaling, and by maintaining functional mitochondria.

INTRODUCTION

Chronic pancreatitis (CP) is a complex inflammatory disorder with progressive, irreversible deterioration, and fibrosis development in pancreas. Recurrent pancreatic injury caused by gallstone diseases (80%) and alcohol abuse (45%) leads to CP. Symptoms include disabling pain in the abdomen, pancreatic insufficiencies, malabsorption, and diabetes. CP can lead to pancreatic cancers (Uc *et al.*, 2016).

Pancreatic acinar cells of exocrine pancreas primarily produce and secrete digestive enzymes. Cholecystokinin is a gut hormone that regulates these enzyme secretions. However, supramaximal doses of cholecystokinin or its analog cerulein (Cer) cause injury to the pancreas, leading to pancreatitis. Ethanol (EtOH) weakens the recovery of injured pancreas. EtOH is metabolized in the pancreas and toxic metabolites like fatty acid ethyl esters (FAEEs), acetaldehyde, and byproducts like reactive oxygen species (ROS) are formed. Increased ROS production causes oxidative stress in the pancreas (Apte *et al.*, 1998). Cer induced pancreatitis is indicated by elevated levels of digestive enzymes and inflammatory cytokines in the serum (Deng *et al.*, 2005). An important mechanism initiating the entire inflammatory response is the up-regulation of genes encoding the secreted

*Corresponding Author
Geetha Arumugam, Dr. Ambedkar Government Arts College, Vyasarpadi,
Chennai, India. E-mail: geethav21 @ yahoo.co.in

mediators like cytokines and chemokines. It takes place by the activation of nuclear factor-κB (NF-κB), a transcription regulator (Chen *et al*., 2018).

Acinar cells have high rate of protein synthesis and so are typically abound in endoplasmic reticulum (ER). ER is involved in the assembly as well as folding of proteins. This function demands optimal redox conditions and calcium concentration. ER is a major intracellular calcium store. Various pathophysiological stimuli, like alcohol and ROS, through changes in calcium concentration lead to the build-up of abnormally folded proteins causing ER stress (Barrera *et al*., 2018; Pandol *et al*., 2010; Zeeshan *et al*., 2016). A stress response called unfolded protein response (UPR) is initiated in the ER with the involvement of various stress sensing proteins like protein kinase RNA-like ER kinase (PERK), activating transcription factor 6 (ATF6), and inositol-requiring enzyme 1 (IRE1). Generally, these proteins are kept inactive by a 78 kDa glucose-regulated protein (GRP78). Their downstream signaling pathways include activating transcription factor 4 (ATF4), CCAAT-enhancer-binding protein homologous protein (CHOP), and X-box binding protein 1 (XBP1) which are aimed to restore homeostasis. However, if prolonged UPR and ER stress exist, homeostasis fails, leading to cytotoxic cellular damage (Cao and Kaufman, 2014; Chakrabarti *et al*., 2011; Lugea *et al*., 2015; Ye *et al*., 2010).

Acinar cells are rich in mitochondria as secretion is energy-intensive. Among various organelles that interact with the ER, mitochondria are important. ER stress culminates in the release of calcium into the mitochondria (Marchi *et al*., 2014). Mitochondrion is very sensitive to ensuing oscillatory increases in calcium levels and to ROS produced by alcohol metabolites (Trumbeckaite *et al*., 2013).

Mitochondrial complex-1 is the prime component in the respiratory chain (ETC) of mitochondria. It transfers electrons from reduced nicotinamide adenine dinucleotide (NADH) to coenzyme Q leading to adenosine triphosphate (ATP) synthesis. Complex-1 is well recorded to be both an intracellular source and a target of ROS (Clemens *et al*., 2014).

An ROS-generating mitochondrion can activate NLRP3 inflammasome, a multiprotein complex. NLRP3 can recognize damage associated molecular patterns generated by damaged mitochondria, serving as a signaling platform for the activation of caspase-1 and release of pro-inflammatory cytokines, interleukin-1β and interleukin-18. It is a key inflammasome involved in different inflammatory diseases, causing an inflammatory cell death. Mitochondria-induced NLRP3 inflammasome activation is implicated in inflammation (Gurung *et al*., 2015; Zhou *et al*., 2011).

Glycyrrhizin (GZ) ($C_{42}H_{62}O_{16}$, 822.942 g/mol), a triterpene saponin, is a major constituent in licorice root (*Glycyrrhiza glabra*). GZ is widely used for treating peptic ulcers, hepatitis and to improve liver function. It is also used as anti-inflammatory, anti-oxidative, and immunomodulatory agent (Li *et al*., 2014).

CP is an increasingly common disease lacking a specific targeted therapy. This study is intended to construct a multi-targeted treatment approach with the potent anti-oxidant, GZ, against EtOH and Cer-induced CP in rats. The focus being, mitigation of inflammation, oxidative stress and calcium overload in mitochondria, and ER stress amelioration.

MATERIALS AND METHODS

Chemicals

RNA later (Cat. #R0901) was procured from Sigma-Aldrich (Saint Louis, MO). GZ was obtained from Tokyo chemical industry chemicals (Chennai, India). Fura-2AM was from Merck (Mumbai, India). Alpha amylase and lipase kits were purchased from Coral Clinical Systems (Goa, India). Cer (product No.C9026-1MG) was from Sigma-Aldrich (Saint Louis, MO).

Experimental animals

Male albino Wistar rats (175–200 g) were housed in polyethylene cages on a 12 hours' light and dark cycle at a temperature of 25°C and humidity between 60% and 70%. Rats were given normal chow diet and water throughout acclimatization. The experimental design was reviewed and validated by the Institutional Animal Ethics Committee XIX/VELS/PCOL/06/2000/CPCSEA/IAEC/03.10.2016.

Induction of pancreatitis using EtOH and Cer

After a week of acclimatization, rats were grouped into four groups (six rats a group) as follows:

Group 1 (Control): normal chow diet and water *ad libitum* all through the 5-week study period (including acclimatization).

Group 2 (GZ control): normal chow diet and water *ad libitum* for 5 weeks and GZ at a dose of 10 mg/kg bodyweight, daily and orally for the last 3 weeks.

Group 3 (EtOH + Cer): isocaloric diet with ethanol (0%–36%) for 4 weeks and an IP injection of Cer (20 μg/kg body weight) three times per week for the last 3 weeks.

Group 4 (EtOH + Cer + GZ): isocaloric diet with ethanol (0%–36%) for 4 weeks, an IP injection of Cer (20 μg/kg body weight) three times per week for the last 3 weeks, along with the administration of GZ, at a daily oral dose of 10 mg/kg bodyweight, for the last 3 weeks.

After the study period, rats were fasted overnight, anesthetized using ether, and euthanized by cervical decapitation. Immediately blood was drawn, plasma and serum were separated and stored at 4°C until further analyses. Pancreas was excised and a portion of it was preserved in RNA later for quantitative polymerase chain reaction (qPCR) analysis.

Histopathological evaluation of pancreatitis

A portion of excised pancreas was cleansed with cold saline (0.9%) and then in formal saline (1:10) for 24 hours. The specimens were treated with alcohol, methyl benzoate and firmed up in paraffin wax. Tissue was then cut into 5 μm thickness and stained with hematoxylin and eosin for microscopic evaluation at 400× magnification.

Pancreatic mitochondrial isolation

Mitochondria was isolated from pancreatic tissue using mitochondria isolation kit for tissue (ab110168) obtained from Abcam (Cambridge, MA). Briefly, differential centrifugation of homogenized tissue samples was conducted (SPIN 1: 1,000 g 10 minutes 4°C for nuclei, SPIN 2: 12,000 g 15 minutes 4°C and repeatedly at 12,000 g for 15 minutes for mitochondria). Initially, the supernatant after first spin was segregated from nuclei and whole cells. It was then centrifuged again to achieve pellet rich in

mitochondria. Concentration of protein in isolated mitochondria was quantified by Bradford protein assay (Bradford, 1976).

Biochemical Investigations

Determination of extent of pancreatic injury and cellular oxidative stress

Extent of pancreatic injury was monitored through activities of amylase and lipase using assay kits AMY(DS):01(P), LIP(UV):01(P), respectively. Besides, oxidative stress was measured through estimations of peroxide content and total antioxidant capacity (TAC). Their ratio oxidative stress index (OSI) was then calculated. The total peroxide content in plasma was estimated by ferrous oxidation-xylenol orange assay (Harma and Erel, 2003; Miyazawa, 1989). TAC was measured using 2,2'-azino-bis (3-ethyl benzothiazoline-6-sulfonic acid) method (Miller *et al.*, 1993).

Assessment of neutrophil infiltration and other inflammatory mediators

Myeloperoxidase (MPO) was extracted from homogenized pancreas and its activity was assayed (Bradley *et al.*, 1982). Serum levels of caspase-1 were estimated by an assay kit, ab39470 from Abcam, Cambridge, MA. Pro-inflammatory cytokines: interleukin-1β was assayed by an ELISA Kit, ab100767 from Abcam, Cambridge, MA, whereas interleukin-18 was estimated by an ELISA Kit, KRC2341 from Thermo Fisher scientific, Mumbai, India were determined.

Determination of mRNA expression of NF-κB and UPR components in ER stress by qPCR analysis

To perform qPCR, pancreas samples were initially processed for RNA isolation followed by conversion to cDNA. First, entire RNA was extracted by using trizol (Chomzynski and Mackey, 1995). RNA was then quantified using a spectrophotometer and the purity of the sample was determined using A260/280 readings. Samples were run on RNA gel to check for DNA contamination after being treated with DNase I from New England Biolabs (Catalogue#M0303S). RNA was converted to cDNA using cDNA reverse transcription kit from Thermo Fisher scientific, Mumbai, India (Catalogue#4368814). The qPCR analysis was performed using specific primer sequences (Table 1) synthesized at Eurofins genomics, Bangalore, India using Oligo perfect primer designer obtained from Thermo Fisher scientific, Mumbai, India. qPCR was performed on Stratagene Mx3000P PCR machine from Agilent technologies (Santa Clara, CA) using SYBR Green premix (Catalogue#RR420A) purchased from Takara Bio Inc, Japan. A two-step real time PCR with initial denaturation at 95°C for 10 minutes, followed by denaturation

for about 30 seconds and annealing at 60°C for 60 seconds was performed. qPCR data was collected and analyzed on MxPro Software from Agilent technologies (Santa Clara, CA). Data was normalized using the comparative Ct values.

Determination of functional capacity of mitochondria

Determination of mitochondrial calcium $[Ca^{2+}]_m$

It was measured by changes in the intensity of fluorescence of mitochondrial isolates, loaded with a ratiometric calcium indicator, fura-2 AM. Mitochondrial isolates were dispersed in 0.25 M sucrose containing 1 mM EGTA and 20 mM Tris (pH 7.4). Then they were loaded with 10 μM fura-2 AM by incubating for 10 minutes at room temperature.

1 mg of fura-2 AM dissolved in 1 ml dimethyl sulfoxide was used as stock solution of fura-2 AM. For use, an aliquot of stock solution was diluted to 10 μM in modified Hanks' balanced salt solution (HBSS with Ca2+) immediately before loading. HBSS contains 137 mM of NaCl, 5.37 mM of KCl, 0.81 mM of $MgSO_4$, 0.44 mM of KH_2PO_4, 0.37 mM of Na_2HPO_4, 1.37 mM of $CaCl_2$, 5.56 mM of glucose (pH was adjusted to 7.2 with 10 mM 4-(2-hydroxyethyl)-1-piperazineethane sulfonic acid) (Lash and Jones, 1993). The mitochondrial suspensions were washed to remove excess fura-2 AM for measurement on a Jobin Yvon Fluorolog-3-11 spectrofluorometer with excitation wavelengths at 340 nm and 380 nm, emission wavelength at 510 nm as described before (Hotta *et al.*, 2001; Trenker *et al.*, 2008). Any change in the intramitochondrial free Ca2+ was measured as 340/380 ratio. The calcium concentrations from mitochondrial isolates of different experimental groups were calculated and expressed in nM by conversion of ratio values (Grynkiewicz *et al.*, 1985).

Determination of mitochondrial dysfunction

Mitochondrial dysfunction was assessed by measuring its complex-1 activity using enzyme activity microplate assay kit (ab109721) obtained from Abcam (Cambridge, MA). This assay measures the NADH-dependent activity of complex-1 at OD 450 nm. The activity was expressed in terms of percentage activity of control, similar to that described previously for liver (Mukhopadhyay *et al.*, 2014) and heart (Hao *et al.*, 2015).

Determination of mitochondrial oxidative stress

Mitochondrial oxidative stress was assessed through estimations of reduced glutathione (GSH), glutathione peroxidase (GPx), superoxide dismutase (SOD), catalase (CAT), malondialdehyde (MDA), and 4-hydroxynonenal (4-HNE) levels. GSH level was determined according to Moron *et al.* (1979). Gpx was assayed as per Flohe and Gunzler. (Flohé and Günzler, 1984). Activity of SOD was estimated according to Kakkar *et al.* (1984). Activity of CAT was kinetically measured at 240 nm (Aebi, 1984).

Thiobarbituric acid-reactive substances (TBARS) assay was used to assess MDA production (Draper and Hadley, 1990). To measure 4-HNE, the mitochondrial fraction was allowed to react with dinitrophenylhydrazine (DNPH), mixed thoroughly and set aside for 1 hour, to derivatize 4-HNE in the sample. Then the formed adduct of 4-HNE and DNPH was extracted thrice with hexane and evaporated to dryness at 40°C. After cooling, 1 ml methanol was then added to all the samples and absorbance was measured at 350 nm using spectrophotometer (Kinter *et al.*, 1994).

Table 1. Details of forward and reverse primers used in real-time PCR analysis.

Gene	Forward primer sequence	Reverse primer sequence
β-actin	5′-CACCAACTGGGACGACAT-3′	5′-ACAGCCTGGATAGCAACG-3′
ATF4	5′-TGAAAGAGAAGGCAGATT-3′	5′-TGAAAGAGAAGGCAGATT-3′
CHOP	5′-TGTTCTCTATTCGTTCCTAA-3′	5′-CCACCATCCTGAACTATT-3′
GRP78	5′-AATCAAGGTCTACGAAGG-3′	5′-AACACTGGTCCAACTAAG-3′
XBP1	5′-AACCTCTTAGATGACTTCCA-3′	5′-AGGCTGAACGATAACTGT-3′
NF-kB	5′-CAATCTTGATGTCATTCG-3′	5′-AAGTGTAATCCAATAGCA-3′

Statistical analysis of data

Statistical Package for the Social Sciences for Windows V.10 was used for the statistical calculations. The significance level was calculated by one-way analysis of variance (ANOVA) and post hoc Bonferroni. P values < 0.05 were reported significant. Spearman's correlation test was performed to identify the correlation between related data sets. The statistical significance (p-value) of correlation coefficient (r_s) was also determined.

RESULTS

Effect of GZ on altered histology of pancreas

Figure 1 depicts sections of pancreatic tissue (400×) from various study groups stained with hematoxylin and eosin. Pancreatic tissue from group 1 and group 2 rats showed no significant pathological manifestations of disease (Fig. 1A and B). In the sections of pancreatic tissue from EtOH and Cer given group 3 rats, a prominent infiltration by neutrophils indicating inflammation and mild fibrosis was observed (Fig. 1C). Pathological alterations caused by EtOH and Cer in the tissue architecture of pancreas were found to be ameliorated in GZ co-administered group 4 rats (Fig. 1D).

Effect of GZ on extent of pancreatic injury and cellular ROS

Amylase and lipase activities in serum were found elevated significantly upon administration of EtOH and Cer, compared to control. GZ co-administration found to have restored these levels significantly. These enzyme activities from all the four experimental groups were tabulated in Table 2 along with cellular oxidative stress and ROS through estimations of plasma total peroxide content, TAC and OSI.

Effect of GZ on neutrophil infiltration and release of inflammatory mediators

Pancreatic MPO activity and serum levels of inflammatory caspase-1, interleukin-1 β, and interleukin-18 in all study groups were shown in Table 3. Upon EtOH and Cer administration, levels of all these inflammatory mediators were found increased significantly compared to control. GZ co-administration was observed to reduce these levels significantly. There was no significant change in GZ control groups compared to control.

Effect of GZ on NF-κB expression

mRNA expressions of NF-κB in pancreatic tissues of various groups were shown in Figure 2. Upregulated expression
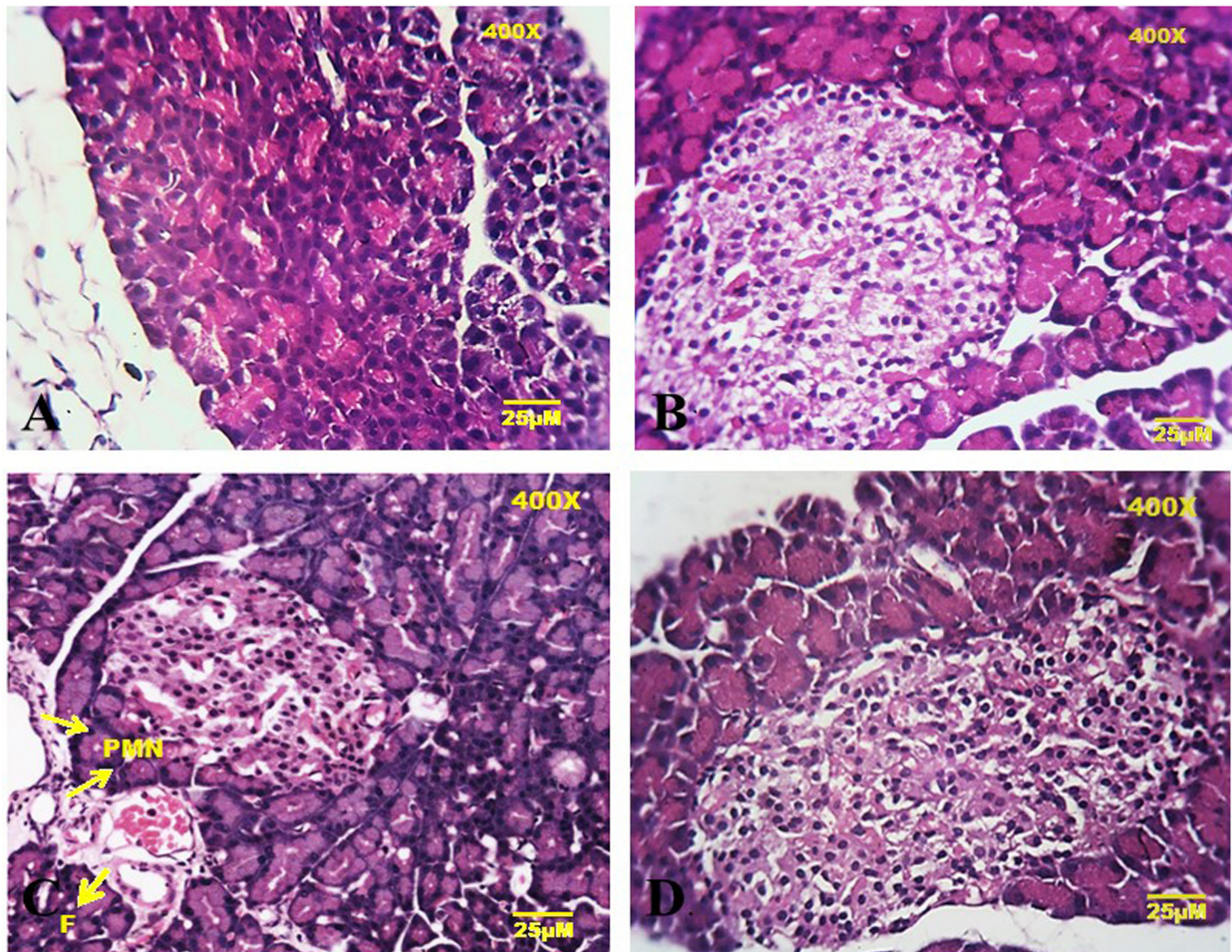

Figure 1. Hematoxylin and Eosin stained (400×) pancreatic sections from all study groups. (A) Control; (B) GZ control; (C) EtOH + Cer induced pancreatitis group revealing polymorphonuclear infiltration(PMN) and fibrosis(F); (D) GZ co-administered group.

Table 2. Effect of GZ treatment on enzyme markers of pancreatic injury and cellular ROS.

Group	Serum lipase (IU/l)	Serum amylase (IU/l)	Total peroxide (mmol/ml)	TAC (mmol trolox eq./l)	OSI
Control	149.1 ± 21.0	1662 ± 204.4	172.3 ± 20.8	332.4 ± 44.54	0.51 ± 0.05
GZ control	148.5 ± 18.0 [NS]	1607 ± 223.3 [NS]	169.8 ± 23.2[NS]	319.9 ± 45.10 [NS]	0.53 ± 0.06[NS]
EtOH + Cer	220.2 ± 28.6*	3118 ± 346*	287.5 ± 34.2*	227.1 ± 29.52*	1.26 ± 0.17*
EtOH + Cer + GZ	137.8 ± 16.6*	2297 ± 349.1*	194.0 ± 21.7*	302.5 ± 33.95*	0.64 ± 0.12*

Values represent mean ± S.D where n=6. Statistical significance was denoted through one-way ANOVA and post-hoc Bonferroni test by comparing control and GZ control; control and EtOH + Cer; EtOH + Cer and EtOH + Cer + GZ.
NS = not significant.
*p <0.05.

Table 3. Effect of GZ treatment on neutrophil infiltration and inflammation.

Groups	MPO (Units/mg protein)	Caspase-1 (pg/ml)	Interleukin-1β (pg/ml)	Interleukin-18 (pg/ml)
Control	2.1 ± 0.23	11.1 ± 1.60	13.75 ± 1.74	177.9 ± 20.4
GZ control	1.98 ± 0.25 [NS]	10.8 ± 1.54 [NS]	13.02 ± 1.62[NS]	169.1 ± 23.5[NS]
EtOH + Cer	3.7 ± 0.50*	96.4 ± 13.3*	29.6 ± 3.87*	302.5 ± 44.1*
EtOH + Cer + GZ	1.95 ± 0.29*	15.2 ± 2.06*	15.3 ± 1.79*	210.6 ± 31.5*

Values represent mean ± S.D where n = 6. Statistical significance was denoted through one-way ANOVA and post-hoc Bonferroni test by comparing control and GZ control; control and EtOH + Cer; EtOH + Cer and EtOH + Cer + GZ.
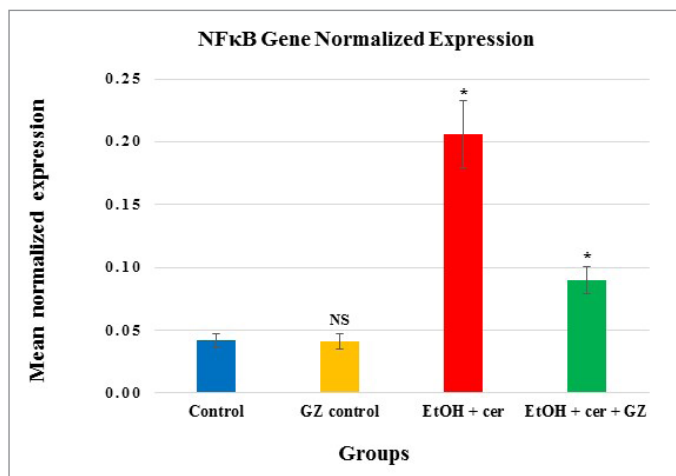NS = not significant.
*p < 0.05.

Figure 2. Gene expression analysis of NF-κB in pancreas studied by qPCR indicating the effect of GZ. *y*-axis represents mean normalized expression values expressed as mean ± S.D, where *n* = 6. Statistical significance was calculated through one-way ANOVA and post-hoc Bonferroni test by comparing control and GZ control; control and EtOH + Cer; EtOH + Cer and EtOH + Cer + GZ; *p < 0.05; NS = not significant.

of NF-κB was seen in EtOH and Cer given group 3 rats than in control. However, in GZ co-administered groups, the expression was found reduced significantly featuring its defense against persistent inflammation in CP.

Effect of GZ on mRNA expression of UPR components in ER stress

mRNA expression levels of UPR components like ATF4, GRP78, CHOP, XBP1 were provided in Figure 3a–d, respectively. In EtOH and Cer given rats, mRNA expression of these UPR genes was found upregulated significantly, indicating the chronically activated ER stress in CP. GZ co-administration was observed to

ameliorate increased expression, underlining its protective effect against pathologic ER stress.

Effect of GZ on functional capacity of mitochondria

Effect of GZ on [Ca $^{2+}$]$_m$

Compared to control groups, the intra-mitochondrial free calcium was observed to be elevated significantly in group 3 rats (Table 4). This increase was not observed upon GZ co-administration, emphasizing attenuation of [Ca $^{2+}$]$_m$ overload by GZ. No significant change was observed in GZ control groups compared to control groups.

Effect of GZ on mitochondrial dysfunction

Complex-1 activities from mitochondrial isolates of various experimental groups were shown in Figure 4. Compared to control groups, pronounced decrease in complex-1 activity of mitochondrial ETC was observed in group 3 rats. It was observed to be restored upon GZ co-administration.

Effect of GZ on mitochondrial oxidative stress

A significant depletion in GSH content and antioxidant enzymes GPx, SOD, CAT was found in the mitochondrial fractions of group 3 rats than in control. Administration of GZ along with EtOH and Cer was recorded to enhance the antioxidative capacity of mitochondria (Table 4) as evidenced from attenuated levels. The lipid peroxidation levels, expressed in terms of TBARS and 4-HNE in mitochondrial fractions of EtOH and Cer given groups were found increased profoundly, compared to control (Table 4). Administration of GZ along with EtOH and Cer restored these levels, further highlighting its anti-oxidative nature.

Spearman's rank correlation analysis

Results of correlation analysis—GRP78 versus 4-HNE; CHOP versus IL-1 β, [Ca $^{2+}$]$_m$ and NF-κB; [Ca $^{2+}$]$_m$ versus TBARS,
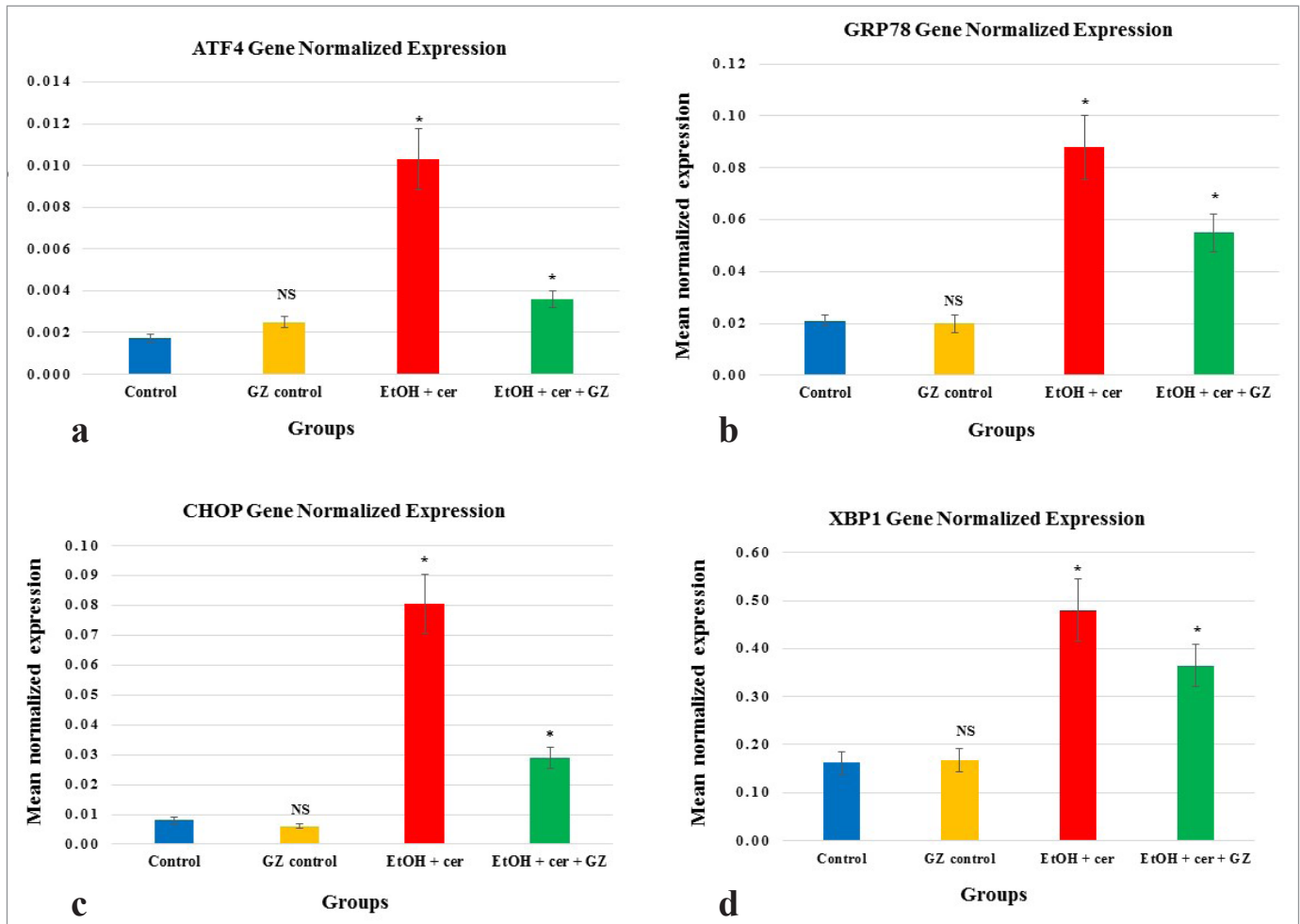
Figure 3. (a) Gene expression analysis of UPR components—ATF4 in pancreas, studied by qPCR indicating the effect of GZ. y-axis represents mean normalized expression values expressed as mean ± S.D, where $n = 6$. Statistical significance was calculated through one-way ANOVA and post-hoc Bonferroni test by comparing control and GZ control; control and EtOH + Cer; EtOH + Cer and EtOH + Cer + GZ; *p <0.05; NS = not significant. (b) Gene expression analysis of UPR components—GRP78 in pancreas, studied by qPCR indicating the effect of GZ. y-axis represents mean normalized expression values expressed as mean ± S.D, where $n = 6$. Statistical significance was calculated through one-way ANOVA and post-hoc Bonferroni test by comparing control and GZ control; control and EtOH + Cer; EtOH + Cer and EtOH + Cer + GZ; *$p < 0.05$; NS = not significant. (c) Gene expression analysis of UPR components—CHOP in pancreas, studied by qPCR indicating the effect of GZ. y-axis represents mean normalized expression values expressed as mean ± S.D, where $n = 6$. Statistical significance was calculated through one-way ANOVA and post-hoc Bonferroni test by comparing control and GZ control; control and EtOH + Cer; EtOH + Cer and EtOH + Cer + GZ; *$p < 0.05$; NS = not significant. (d) Gene expression analysis of UPR components—XBP1 in pancreas, studied by qPCR indicating the effect of GZ. y-axis represents mean normalized expression values expressed as mean ± S.D, where $n = 6$. Statistical significance was calculated through one-way ANOVA and post-hoc Bonferroni test by comparing control and GZ control; control and EtOH + Cer; EtOH + Cer and EtOH + Cer + GZ; *$p < 0.05$; NS = not significant.

Table 4. Effect of GZ treatment on mitochondrial oxidative stress and $[Ca^{2+}]_m$.

Group	GSH (mg/g protein)	Gpx (nM GSH oxidized/ minute/mg protein)	SOD (units/mg protein)	CAT (µ mol H_2O_2 consumed/minute/mg protein)	TBARS (nM/ mg protein)	4-HNE (µM/g protein)	$[Ca^{2+}]_m$ (nM)
Control	4.8 ± 0.61	122.3 ± 16.38	6.9 ± 0.70	5.1 ± 0.57	8.6 ± 1.075	0.040 ± 0.006	91.63 ± 11.08
GZ control	4.6 ± 0.60[NS]	119.7 ± 15.20[NS]	6.7 ± 0.73[NS]	4.8 ± 0.61[NS]	9.2 ± 1.104[NS]	0.035 ± 0.004[NS]	93.7 ± 11.99[NS]
EtOH +Cer	2.7 ± 0.39*	79.4 ± 11.43*	3.6 ± 0.42*	2.6 ± 0.26*	13.1 ± 1.89*	0.132 ± 0.017*	168.9 ± 20.09*
EtOH +Cer+ GZ	3.9 ± 0.43*	109.3 ± 14.20*	5.2 ± 0.62*	4.0 ± 0.48*	10.4 ± 1.16*	0.067 ± 0.007*	79.5 ± 9.14*

Values represent mean ± S.D where $n = 6$. Statistical significance was denoted through one-way ANOVA and post-hoc Bonferroni test by comparing control and GZ control; control and EtOH + Cer; EtOH + Cer and EtOH + Cer + GZ.
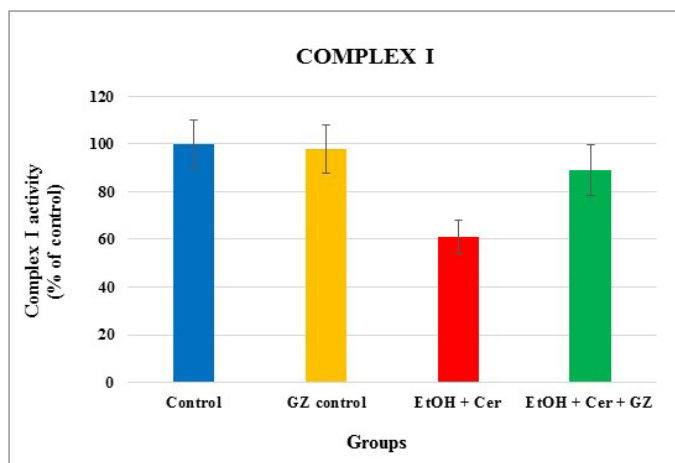NS = not significant.
*p <0.05.

Figure 4. Complex-1 activity from mitochondrial isolates of various experimental groups indicating the attenuation of EtOH +Cer induced mitochondrial dysfunction by GZ. Values of GZ control, EtOH + Cer and EtOH + Cer + GZ were expressed as percentage activity of control.

Table 5. Spearman's rank correlation for different variables of study.

Parameter	r_s	P
GRP78 versus 4-HNE	0.78	<0.05
CHOP versus IL-1β	0.77	<0.05
CHOP versus $[Ca^{2+}]_m$	0.89	<0.001
CHOP versus NF-κB	0.81	<0.025
$[Ca^{2+}]_m$ versus complex-1	−0.82	<0.025
$[Ca2+]_m$ versus TBARS	1.00	<0.001
$[Ca^{2+}]_m$ versus GSH	−0.71	0.05

r_s = spearman's correlation coefficient; P = statistical significance.

GSH and complex-1 were presented in Table 5. A strong negative correlation was seen between $[Ca^{2+}]_m$ and GSH; $[Ca^{2+}]_m$ and complex-1. And a strong positive correlation was observed among all the other data sets compared.

DISCUSSION

In the current study, protective effect of GZ against organelle dysfunction and chronic inflammation in CP was investigated in detail. These are the key pathological events for the progression of pancreatitis. No specific therapies for pancreatitis have been developed effectively so far except the supportive therapy (Frola *et al.*, 2019). CP was induced in rats by repeated dose of Cer combined with a sensitizing agent, EtOH. Cer hyperstimulation induces pancreatic injury in rats and EtOH aggravates this pathological effect towards CP, with clinical presentations like persistent inflammation (Deng *et al.*, 2005).

The functioning of pancreatic acinar cells depends on coordinated actions of ER and mitochondria. Previous studies clearly indicated that their functional ability has been disturbed in pancreatitis (Gukovskaya *et al.*, 2016). Physiologically, pancreatic digestive enzymes are synthesized in ER of pancreatic acini, transported as inactive pro-enzymes and get activated only in the small intestine. Accurate protein processing by ER is extremely important, to avoid any premature activation of pancreatic enzymes in acinar cells itself. Cytosolic calcium concentration

and calcium release from intracellular calcium pools (primarily ER), in response to hormonal stimuli is a signaling mechanism for this process. Metabolites of EtOH like FAEE and other fatty acids, along with Cer were shown to induce gradual release of calcium from ER (called calcium store depletion) leading to pathological calcium signaling patterns (Criddle *et al.*, 2006). It can induce premature activation of pancreatic enzymes and pancreatic tissue destruction. Thus, injured pancreatic acini facilitate the release of pancreatic enzymes into the blood stream. The enzyme markers of EtOH and Cer-induced pancreatic injury are lipase and amylase activities, which are generally monitored in serum (Frulloni *et al.*, 2005). In this investigation, increased serum levels of these enzymes were found in EtOH and Cer-given group 3 rats and these serological alterations were found to be ameliorated with GZ co-administration.

ER, an important organelle for protein folding and calcium storage; mitochondria, which interpret intracellular calcium signals by taking up and releasing calcium are the two key cellular organelles most disordered in EtOH and Cer-induced injury (Lugea *et al.*, 2015). Administration of EtOH can perturb ER homeostasis, by imparting aggregation of improperly folded nascent polypeptides, causing substantial activation of UPR and ER stress. Acinar cells may be prompted to injury and death in due course (Criddle *et al.*, 2007). Oxidative stress could be a probable mechanism behind the induction of pancreatic ER stress by EtOH. A study by Waldron *et al.* (2018) has shown that EtOH through its oxidative effect caused deformities in the structure of ER, promoting ER stress-related pathology in mouse pancreas. And all these pathological changes are further aggravated in response to Cer. Chronic ER stress is well recorded to be a primary cellular pathomechanism of pancreatitis.

In this study, ER stress was studied by monitoring the mRNA expressions of its UPR components—GRP78, ATF4, CHOP, XBP1. ATF4 is involved in the transcription of genes needed to rebuild ER homeostasis and activates the genes encoding antioxidative stress responses. ATF4 also activates genes responsible for the regulation of intracellular redox status and GSH synthesis. CHOP/GADD153, a transcription factor of ER stress is a 29 kDa protein which is required in apoptosis promoted by ER stress (Lugea *et al.*, 2015). Elevated CHOP is related to uncontrolled inflammation as it regulates cytokine production and promotes increased number of inflammatory cells. CHOP also causes the production of interleukin-1 β by triggering caspase-1 through caspase-11, leading to inflammatory stress responses (Nishitoh, 2012). Protein processing in ER is executed by various chaperones. GRP78 is an abundant ER-specific chaperone belonging to HSP70 family and this protein inactivates other chaperones like PERK, IRE1, and ATF6, which relate ER stress to UPR stimulation. When unfolded proteins pile up, GRP78 leaves the three receptors leading to the stimulation of these receptors and triggering of respective UPR pathways. GRP78 is very sensitive to ER stress (Chaudhari *et al.*, 2014). XBP1 is an active factor of transcription for the production of GRP78. Overexpression of mRNA level of XBP1 was documented previously in CP. Stimulation of IRE1/XBP1 pathway is a cellular stress response to reinstate protein processing in ER (Sah *et al.*, 2014). Together, the UPR mechanisms alleviate ER stress to maintain ER homeostasis. It is very important for a functional acinar cell during both normal

and diseased states. But if the ER stress is not rectified, persistent stimulation of the UPR takes place.

In the study, a sustained up-regulation of mRNA expressions of all the four UPR components—ATF4, CHOP, GRP78, and XBP1 was seen in EtOH and Cer-given group, which revealed the existence of persistent ER stress. GZ co-administration significantly reduced the EtOH and Cer-induced ER stress as observed from downregulated expression of these genes in GZ co-administered rats. Lugea et al. (2015) hypothesized that pancreas initiates this adaptive UPR to reduce the ER stress generated by alcohol. But when it is beyond the protective capacity of UPR, it progresses to CP. Our study highlighted the pancreas-protective effect of GZ in EtOH and Cer-induced CP with UPR as a definitive target.

Generally, acinar cells contain high number of mitochondria as energy source for the synthesis of digestive enzymes. Pancreatic mitochondria are more susceptible intracellular targets to EtOH-induced injury. Both non-oxidative and oxidative metabolism of alcohol disturbs pancreatic mitochondrial functions and causes acinar cell death by aberrant calcium signaling (Clemens et al., 2014). As the excess calcium released from ER, in response to alcoholic metabolites is received by pancreatic mitochondria, sustained elevation of mitochondrial calcium takes place. Mitochondria depict the primary intracellular origin for the production of ROS. Physiologically, many superoxides and hydrogen peroxides are formed during mitochondrial ETC. Mitochondrial ROS further promotes calcium release from nearby ER and increases $[Ca^{2+}]_m$ accumulation, initiating a positive feedback cycle. Excessive flow of calcium to mitochondria leads to calcium stimulated oxidative damage to mitochondria, failure of ATP production, energy deprivation, and cellular necrosis (Cao and Kaufman, 2014). Toxic accumulation of ROS is usually countered by GSH, SOD, and CAT. To investigate the mitochondrial oxidative stress, GSH, GPx, SOD, and CAT were monitored. Oxidative stress disrupts mitochondrial membrane, as shown by excess lipid peroxidation products like TBARS and 4-HNE, affecting permeability. A significant decrease in the levels of antioxidants accompanied by an increase in lipid peroxidation products was noticed in EtOH and Cer-given group 3 rats than in control. Co-administering GZ restrained these changes. Reduced enzyme activities of SOD and GPx lead to oxidative stress in mitochondria (Zang et al., 2007). Alteration in the mitochondrial function is one of the mechanisms for the onset and progression of pancreatitis. It has been observed that, GZ treatment can be a good strategy to target mitochondria, in order to locally scavenge ROS at their site of origin itself. mitoquinone and 10-(6'-plastoquinonyl) decyltriphenylphosphonium are the other mitochondria targeted antioxidants proved to be effective against pancreatitis, by acting as scavengers of ROS (Huang et al., 2015; Weniger et al., 2016).

ER stress and mitochondrial oxidative stress are interlinked phenomena regulated through calcium. Calcium serves as a second messenger for many cellular processes. To determine the $[Ca^{2+}]_m$ concentration, fura-2AM which is a membrane permeable, non-invasive, ratiometric indicator was used. It can accumulate to a variable extent when loaded onto mitochondrial isolates (Sheu and Sharma, 1999). Excitation wavelengths used to determine Bound-Ca^{2+} fura-2 AM and free-Ca^{2+} fura-2 AM are 340 nm and 380 nm, respectively. Fura-2 AM emits at 510 nm for both the states. The ratio of 510 nm to 340 nm and 510 nm to

380 nm indicates the calcium levels (Grynkiewicz et al., 1985). In the study, $[Ca^{2+}]_m$ concentration in EtOH and Cer-given group 3 rats was found increased significantly than in control and GZ co-administered group 4 rats. Although modest increase in $[Ca^{2+}]_m$ concentrations enhances enzymatic activity and subsequent ATP synthesis, excessive $[Ca^{2+}]_m$ load may disable ATP synthetic pathways (Brookes et al., 2004). The results showed attenuation of $[Ca^{2+}]_m$ overload by GZ. Odinokova et al. (2009) suggested that both the ROS and calcium in mitochondria regulate the functional status of acinar cells during pancreatitis and further highlighted that stabilizing mitochondria against such functional loss may be a good approach to reduce the severity of pancreatitis. Mitochondrial cytochrome C is released under the influence of $[Ca^{2+}]_m$ overload and excess ROS. The loss of cytochrome C has been shown to inhibit the ETC leading to mitochondrial dysfunction.

Mitochondrial dysfunction was assessed through complex-1 activity in the isolated mitochondria. Complex-1 is the gate keeper of ETC and is reported to be severely affected in oxidative stress (Wu et al., 2015). Early organ specific pancreatic mitochondrial dysfunction in Cer-induced pancreatitis was described by various studies (Trumbeckaite et al., 2013). EtOH affects the mitochondrial functioning through its oxidative metabolite acetaldehyde, which destabilizes the ETC (Manzo-Avalos and Saavedra-Molina, 2010). In this study, marked inhibition of mitochondrial complex-1 activity was observed upon EtOH and Cer administration and it was found to be restored with GZ co-administration. Mitochondrial compex-1 is positioned in the inner membrane of mitochondria, which is prone to lipid peroxidation. The formed 4-HNE can produce HNE-protein adducts with complex-1, affecting its function. It was illustrated in mitochondrial isolates of diabetic rat kidney by Wu et al. (2015). Sun et al. (2016) demonstrated that chronic alcohol feeding to rats increases the 4-HNE levels in liver mitochondria leading to impaired functioning of respiratory complexes. The defective complexes of ETC can further exacerbate ROS generation in mitochondria. GZ co-administration prevented the loss in activity of complex-1 and this might be by modulating 4-HNE level, underlining its protection against mitochondrial damage in CP.

Sustained ER stress activates inflammatory pathways through chronic NF-κB activation in CP (Sah et al., 2014). We observed an up-regulated mRNA expression of NF-κB in EtOH and Cer-given group and, GZ co-administration was found to counteract it. NF-κB is held ineffective by IκBα, an inhibitor of NF-κB in normal cells. Many studies have shown ER stress to downregulate IκBα leading to NF-κB activation. EtOH also causes activation of NF-κB directly through the activation of protein kinase C in pancreatic acini (Gukovskaya et al., 2004). NF-κB integrates ER stress with pro-inflammatory response through a protein called tumor necrosis factor α receptor-associated factor2 that activates NF-kB, promoting its nuclear translocation. The activated NF-κB promotes expression of pro-inflammatory cytokines and chemokines increasing the severity of pancreatitis. It has also been well documented that, inhibition of NF-κB improves pancreatic function (Huang et al., 2013).

Correlation analysis is a statistical method to find out the strength of a relationship between two sets of data. The Spearman's rank correlation was measured between GRP78 versus 4-HNE; CHOP versus IL-1β, $[Ca^{2+}]_m$; $[Ca^{2+}]_m$ versus complex-1,

TBARS and GSH; CHOP versus NF-κB. Rs value, and its statistical significance level based on exact critical probability (p) values were calculated. Considering the small *p* values, the null hypothesis was rejected and the relationship between compared datasets was found significant. In the study, a positive correlation was noticed between GRP78 versus 4-HNE and CHOP versus IL-1β, $[Ca^{2+}]_m$. A correlated effect was observed between ER stress and mitochondrial dysfunction, the key mechanisms contributing to the pathobiology of CP.

Moreover, histological observations in the study evidenced a prominent neutrophil infiltration and mild fibrosis in pancreatic sections of EtOH and Cer-given groups which is a characteristic feature of CP. This was found to be counteracted by GZ, as observed in pancreatic sections of GZ co-administered rats. The reason behind this excessive inflammatory response in group 3 rats is perhaps the NF-κB activation, as noted in this study. The transcription of NF-κB genes is often activated by cellular ROS (Morgan and Liu, 2011). The attenuation of NF-κB activation by GZ in our study is probably by influencing the cellular ROS levels as shown by total peroxide content, TAC and OSI levels. In a similar study, Morin which is an anti-inflammatory flavone has been found to reduce activation of NF-κB by its anti-oxidant properties (Kim *et al.*, 2010).

ER stress-induced mitochondrial damage and associated ROS also cause activation of NLRP3 inflammasome and associated inflammatory responses that worsen pancreatitis. Mitochondrial ROS was shown to activate NLRP3 inflammasome directly. NLRP3 inflammasome is assembled from its component proteins, namely, NLRP3 sensor, apoptosis-associated speck-like protein containing a caspase activation and recruitment domain and caspase-1. Upon activation, caspase-1 cleaves pro-interleukin1β and pro-interleukin 18 into inflammatory cytokines interleukin-1β and interleukin-18 that mediates pancreatic tissue injury (Liu *et al.*, 2018). In the present investigation, the serum levels of caspase-1, interleukin-1β, and interleukin-18 were noticed to be increased in EtOH and Cer-given rats and GZ co-administration observed to counteract these modifications, highlighting its ability to reduce the disease severity. The energy deficits with mitochondrial complex-1 impairment and mitochondrial oxidative stress, accompanied by excessive unfolded ER proteins impair ER-mitochondrial cooperation, promoting inflammatory responses. The basic therapy for CP is the treatment of pain and underlying inflammation. Many anti-inflammatory agents like thalidomide, panhematin, montelukast, dantrolene were documented to be effective against pancreatitis (Sah and Saluja, 2011).

CONCLUSION

From the study, it could be conjectured that GZ ameliorates the pancreatic impairment in CP by targeting the UPR, NF-κB mediated NLRP3 inflammasome activation, and cytokine maturation, in addition to preserving the functional ability of the mitochondria. GZ is observed to influence the heat shock protein GRP78. Its potential to influence other molecular chaperones like HSP27, HSP60, HSP70, and HSP90 known to be involved in pancreatic pathophysiology, could hold a valuable therapeutic potential. An *in silico* docking study could be performed to compute the ability of GZ to interact with UPR, NLRP3 component proteins and heat shock proteins, to further confirm the drug-like property of GZ.

CONFLICTS OF INTEREST

PUBLISHER'S NOTE

This journal remains neutral with regard to jurisdictional claims in published institutional affiliation.

REFERENCES

Aebi H. Catalase *in vitro*. Methods Enzymol, 1984; 105:121–6.

Apte MV, Haber PS, Norton ID, Wilson JS. Alcohol and the pancreas. Addict Biol, 1998; 3(2):137–50.

Barrera K, Stanek A, Okochi K, Niewiadomska Z, Mueller C, Ou P, John D, Alfonso AE, Tenner S, Huan C. Acinar cell injury induced by inadequate unfolded protein response in acute pancreatitis. World J Gastrointest Pathophysiol, 2018; 9(2):37.

Bradford MM. A rapid and sensitive method for the quantitation of microgram quantities of protein utilizing the principle of protein-dye binding. Anal Biochem, 1976; 72(1–2):248–54.

Bradley PP, Priebat DA, Christensen RD, Rothstein G. Measurement of cutaneous inflammation: estimation of neutrophil content with an enzyme marker. J Invest Dermatol, 1982; 78(3):206–9.

Brookes PS, Yoon Y, Robotham JL, Anders MW, Sheu SS. Calcium, ATP, and ROS: a mitochondrial love-hate triangle. Am J Physiol Cell Physiol, 2004; 287(4):C817–33.

Cao SS, Kaufman RJ. Endoplasmic reticulum stress and oxidative stress in cell fate decision and human disease. Antioxid Redox Signal, 2014; 21(3):396–413.

Chakrabarti A, Chen AW, Varner JD. A review of the mammalian unfolded protein response. Biotechnol Bioeng, 2011; 108(12):2777–93.

Chaudhari N, Talwar P, Parimisetty A, Lefebvre d'Hellencourt C, Ravanan P. A molecular web: endoplasmic reticulum stress, inflammation, and oxidative stress. Front Cell Neurosci, 2014; 8:213.

Chen L, Deng H, Cui H, Fang J, Zuo Z, Deng J, Li Y, Wang X, Zhao L. Inflammatory responses and inflammation-associated diseases in organs. Oncotarget, 2018; 9(6):7204.

Chomzynski P, Mackey K. Modification of the TRI reagent [TM] procedure for isolation of RNA from polysaccharide-and proteoglycan-rich sources. Biotechniques, 1995; 19:942–5.

Clemens DL, Wells MA, Schneider KJ, Singh S. Molecular mechanisms of alcohol associated pancreatitis. World J Gastrointest Pathophysiol, 2014; 5(3):147.

Criddle DN, Gerasimenko JV, Baumgartner HK, Jaffar M, Voronina S, Sutton R, Petersen OH, Gerasimenko OV. Calcium signalling and pancreatic cell death: apoptosis or necrosis? Cell Death Differ, 2007; 14(7):1285–94.

Criddle DN, Murphy J, Fistetto G, Barrow S, Tepikin AV, Neoptolemos JP, Sutton R, Petersen OH. Fatty acid ethyl esters cause pancreatic calcium toxicity via inositol trisphosphate receptors and loss of ATP synthesis. Gastroenterology, 2006; 130(3):781–93.

Deng X, Wang L, Elm MS, Gabazadeh D, Diorio GJ, Eagon PK, Whitcomb DC. Chronic alcohol consumption accelerates fibrosis in response to cerulein-induced pancreatitis in rats. Am J Pathol, 2005; 166(1):93–106.

Draper HH, Hadley M. Malondialdehyde determination as index of lipid Peroxidation. Methods Enzymol, 1990; 186:421–31.

Flohé L, Günzler WA. Assays of glutathione peroxidase. Methods Enzymol, 1984; 105:114–20.

Frola C, Somasundaram M, Hariharan D, Kolaityte V, Mohandas S, Stättner S, Yip VS. The role of surgery in chronic pancreatitis. Eur Surg, 2019; 51(3):114–20.

Frulloni L, Patrizi F, Bernardoni L, Cavallini G. Pancreatic hyperenzymemia: clinical significance and diagnostic approach. JOP, 2005; 6(6):536–51.

Grynkiewicz G, Poenie M, Tsien RY. A new generation of Ca2+ indicators with greatly improved fluorescence properties. J Biol Chem, 1985; 260(6):3440–50.

Gukovskaya AS, Hosseini S, Satoh A, Cheng JH, Nam KJ, Gukovsky I, Pandol SJ. Ethanol differentially regulates NF-κB activation in pancreatic acinar cells through calcium and protein kinase C pathways. Am J Physiol Gastrointest Liver Physiol, 2004; 286(2):G204–13.

Gukovskaya AS, Pandol SJ, Gukovsky I. New insights into the pathways initiating and driving pancreatitis. Curr Opin Gastroenterol, 2016; 32(5):429–435

Gurung P, Lukens JR, Kanneganti TD. Mitochondria: diversity in the regulation of the NLRP3 inflammasome. Trends Mol Med, 2015; 21(3):193–201.

Hao E, Mukhopadhyay P, Cao Z, Erdélyi K, Holovac E, Liaudet L, Lee WS, Haskó G, Mechoulam R, Pacher P. Cannabidiol protects against doxorubicin-induced cardiomyopathy by modulating mitochondrial function and biogenesis. Mol Med, 2015; 21(1):38–45.

Harma M, Erel O. Increased oxidative stress in patients with hydatidiform mole. Swiss Med Wkly, 2003; 133(4142):563–6.

Hotta Y, Ishikawa N, Ohashi N, Matsui K. Effects of SM-20550, a selective Na+-H+ exchange inhibitor, on the ion transport of myocardial mitochondria. Mol Cell Biochem, 2001; 219(1–2):83–90.

Huang H, Liu Y, Daniluk J, Gaiser S, Chu J, Wang H, Li ZS, Logsdon CD, Ji B. Activation of nuclear factor-κB in acinar cells increases the severity of pancreatitis in mice. Gastroenterology, 2013; 144(1):202–10.

Huang W, Cash N, Wen L, Szatmary P, Mukherjee R, Armstrong J, Chvanov M, Tepikin AV, Murphy MP, Sutton R, Criddle DN. Effects of the mitochondria-targeted antioxidant mitoquinone in murine acute pancreatitis. Mediators Inflamm, 2015; 2015:901780

Kakkar P, Das B, Viswanathan PN. A modified spectrophotometric assay of superoxide dismutase. Indian J Biochem Biophys, 1984; 21(2):130–2.

Kim JM, Lee EK, Park G, Kim MK, Yokozawa T, Yu BP, Chung HY. Morin modulates the oxidative stress-induced NF-κB pathway through its anti-oxidant activity. Free Radic Res, 2010; 44(4):454–61.

Kinter M, Robinson CS, Grimminger LC, Gillies PJ, Shimshick EJ, Ayers C. Whole blood and plasma concentrations of 4-hydroxy-2-nonenal in Watanabe heritable hyperlipidemic versus New Zealand White rabbits. Biochem Biophys Res Commun, 1994; 199(2):671–5.

Lash LH, Jones DP. Mitochondrial dysfunction: methods in toxicology. Elsevier, Amsterdam, Netherlands, 1993.

Li JY, Cao HY, Liu P, Cheng GH, Sun MY. Glycyrrhizic acid in the treatment of liver diseases: literature review. Biomed Res Int, 2014; 2014:872139.

Liu Q, Zhang D, Hu D, Zhou X, Zhou Y. The role of mitochondria in NLRP3 inflammasome activation. Mol immunol, 2018; 103:115–24.

Lugea A, Waldron RT, Pandol SJ. Pancreatic adaptive responses in alcohol abuse: role of the unfolded protein response. Pancreatology, 2015; 15(4): S1–5.

Manzo-Avalos S, Saavedra-Molina A. Cellular and mitochondrial effects of alcohol consumption. Int J Environ Res Public Health, 2010; 7(12):4281–304.

Marchi S, Patergnani S, Pinton P. The endoplasmic reticulum–mitochondria connection: one touch, multiple functions. Biochim Biophys Acta, 2014; 1837(4):461–9.

Miller NJ, Rice-Evans C, Davies MJ, Gopinathan V, Milner A. A novel method for measuring antioxidant capacity and its application to monitoring the antioxidant status in premature neonates. Clin Sci, 1993; 84(4):407–12.

Miyazawa T. Determination of phospholipid hydroperoxides in human blood plasma by a chemiluminescence-HPLC assay. Free Radic Biol Med, 1989; 7(2):209–18.

Morgan MJ, Liu ZG. Crosstalk of reactive oxygen species and NF-κB signaling. Cell Res, 2011; 21(1):103–15.

Moron MS, Depierre JW, Mannervik B. Levels of glutathione, glutathione reductase and glutathione S-transferase activities in rat lung and liver. Biochim Biophys Acta, 1979; 582(1):67–78.

Mukhopadhyay P, Rajesh M, Cao Z, Horváth B, Park O, Wang H, Erdelyi K, Holovac E, Wang Y, Liaudet L, Hamdaoui N. Poly (ADP-ribose) polymerase-1 is a key mediator of liver inflammation and fibrosis. Hepatology, 2014; 59(5):1998–2009.

Nishitoh H. CHOP is a multifunctional transcription factor in the ER stress response. J Biochem, 2012; 151(3):217–9.

Odinokova IV, Sung KF, Mareninova OA, Hermann K, Evtodienko Y, Andreyev A, Gukovsky I, Gukovskaya AS. Mechanisms regulating cytochrome c release in pancreatic mitochondria. Gut, 2009; 58(3):431–42.

Pandol SJ, Gorelick FS, Gerloff A, Lugea A. Alcohol abuse, endoplasmic reticulum stress and pancreatitis. Dig Dis, 2010; 28(6):776–82.

Sah RP, Garg SK, Dixit AK, Dudeja V, Dawra RK, Saluja AK. Endoplasmic reticulum stress is chronically activated in chronic pancreatitis. J Biol Chem, 2014; 289(40):27551–61.

Sah RP, Saluja A. Molecular mechanisms of pancreatic injury. Curr Opin Gastroenterol, 2011; 27(5):444.

Sheu SS, Sharma VK. A novel technique for quantitative measurement of free Ca2+ concentration in rat heart mitochondria. J Physiol, 1999; 518(2):577–84.

Sun Q, Zhong W, Zhang W, Zhou Z. Defect of mitochondrial respiratory chain is a mechanism of ROS overproduction in a rat model of alcoholic liver disease: role of zinc deficiency. Am J Physiol Gastrointest Liver Physiol, 2016; 310(3):G205–14.

Trenker M, Fertschai I, Malli R, Graier WF. UCP2/3—likely to be fundamental for mitochondrial Ca 2+ uniport. Nat Cell Biol, 2008; 10(11):1237–40.

Trumbeckaite S, Kuliaviene I, Deduchovas O, Kincius M, Baniene R, Virketyte S, Bukauskas D, Jansen E, Kupčinskas L, Borutaite V, Gulbinas A. Experimental acute pancreatitis induces mitochondrial dysfunction in rat pancreas, kidney and lungs but not in liver. Pancreatology, 2013; 13(3):216–24.

Uc A, Andersen DK, Bellin MD, Bruce JI, Drewes AM, Engelhardt JF, Forsmark CE, Lerch MM, Lowe ME, Neuschwander-Tetri BA, O'Keefe SJ. Chronic pancreatitis in the 21st century-research challenges and opportunities: summary of a National Institute of Diabetes and Digestive and Kidney Diseases Workshop. Pancreas, 2016; 45(10):1365.

Waldron RT, Su HY, Piplani H, Capri J, Cohn W, Whitelegge JP, Faull KF, Sakkiah S, Abrol R, Yang W, Zhou B. Ethanol induced disordering of pancreatic acinar cell endoplasmic reticulum: an ER stress/defective unfolded protein response model. Cell Mol Gastroenterol Hepatol, 2018; 5(4):479–97.

Weniger M, Reinelt L, Neumann J, Holdt L, Ilmer M, Renz B, Hartwig W, Werner J, Bazhin AV, D'Haese JG. The analgesic effect of the mitochondria-targeted antioxidant SkQ1 in pancreatic inflammation. Oxid Med Cell Longev, 2016; 2016:4650489.

Wu J, Luo X, Yan LJ. Two dimensional blue native/SDS-PAGE to identify mitochondrial complex I subunits modified by 4-hydroxynonenal (HNE). Front Physiol, 2015; 6:98.

Ye R, Mareninova OA, Barron E, Wang M, Hinton DR, Pandol SJ, Lee AS. Grp78 heterozygosity regulates chaperone balance in exocrine pancreas with differential response to cerulein-induced acute pancreatitis. Am J Pathol, 2010; 177(6):2827–36.

Zang Q, Maass DL, White J, Horton JW. Cardiac mitochondrial damage and loss of ROS defense after burn injury: the beneficial effects of antioxidant therapy. J Appl Physiol, 2007; 102(1):103–12.

Zeeshan H, Lee G, Kim HR, Chae HJ. Endoplasmic reticulum stress and associated ROS. Int J Mol Sci, 2016; 17(3):327.

Zhou R, Yazdi AS, Menu P, Tschopp J. A role for mitochondria in NLRP3 inflammasome activation. Nature, 2011; 469(7329):221–5.